PLATELET ACTIVE CONCENTRATION PROFILES NEAR GROWING THROMBI

A Mathematical Consideration

JEFFREY A. HUBBELL AND LARRY V. MCINTIRE
Rice University, Biomedical Engineering Laboratory, Houston, Texas 77251

ABSTRACT When blood contacts foreign material surfaces, platelets usually adhere and form aggregates on those surfaces, generating mural thrombi. The mechanism of mural thrombogenesis is not completely understood, but one hypothesis states that the local release of certain platelet-active substances from the platelets composing an initial small thrombus stimulates additional platelet recruitment to that thrombus, resulting in growth of the cell aggregate. The purpose of this paper is to investigate the feasibility of this hypothesis. Concentration profiles of adenosine diphosphate (ADP), thromboxane A_2 (TxA_2), and thrombin were computed in the vicinity of growing model thrombi 10 and 20 μm long. Wall shear rates of 100, 500, and 1,500 s^{-1} were considered for blood flowing through a thin rectangular slit 200 μm wide coated with collagen, a predominant subendothelial protein. The local concentrations of ADP and TxA_2 were marginally large enough to stimulate platelet activation individually, while local thrombin levels can be much greater than required for stimulation. Antithrombin III, a natural thrombin inhibitor, did not significantly reduce the thrombin concentrations, but antithrombin III accelerated by heparin greatly reduced the local thrombin concentrations. The reduced thrombin levels may, however, still be large enough to activate platelets.

INTRODUCTION

When blood contacts a foreign surface, be it the subendothelium of an injured blood vessel (1), an atheromatous plaque in a blood vessel, or an artificial polymeric surface in a prosthetic blood-contacting device (2), blood platelets adhere to and aggregate on that surface. The result of this process, certainly in the case of exposed subendothelium and atheromatous plaque and often in the case of artificial biomaterials, is the formation of mural thrombi, discrete aggregates of platelets at the blood-surface interface.

The formation of these thrombi is beneficial in the case of an injured vessel, for they form a hemostatic plug and arrest bleeding. In the case of an atheromatous plaque or an artificial biomaterial in a blood-contacting device, however, the formation of these thrombi is very detrimental, for they can embolize from the surface and flow downstream to lodge in the circulation of vital organs. This can cause the cessation of blood flow to parts of an organ, resulting in local ischemia. In the most catastrophic of cases, the result is coronary occlusion or stroke.

It is therefore desirable to understand the mechanism of mural thrombogenesis, to perhaps develop an antithrombotic pharmacological treatment or design an artificial organ so as to minimize thrombosis and subsequent embolization. It has been shown that thrombi formed from flowing blood on collagen are elongated parallel to the direction of flow and seem to grow predominantly by addition to the downstream end of the thrombus (3, 4). One proposed mechanism for thrombogenesis is that the adherent platelets, if sufficiently activated by the surface, produce local high concentrations of platelet-active substances, which then activate other platelets flowing nearby (3). These platelets then aggregate with the already adherent platelets, forming a mural thrombus.

Probably the most important of these platelet active substances are adenosine diphosphate (ADP), which is released from the dense granules of the platelet, and thromboxane A_2 (TxA_2) and thrombin, which are enzymatically generated on or near the membrane of the platelet.

ADP is a strong stimulant of platelet activity, causing shape change and reversible aggregation at concentrations from 0.2 to 1.0 μM and irreversible aggregation at concentrations greater than 1.0 μM (5).

Thromboxane A_2, an arachidonic acid metabolite, is one of the most potent stimulators of platelet activity yet described. TxA_2 is unstable in aqueous media and undergoes rapid nonenzymatic hydrolysis to thromboxane B_2, a biologically inactive substance. The half-life of TxA_2 in aqueous solution is 43 s (6). Because of this short half-life, it is difficult to determine what concentrations of TxA_2 are required to stimulate activity. One of the closest TxA_2 analogues, U-46619 (11,9-epoxy-methano analogue of

BIOPHYS. J. © Biophysical Society · 0006-3495/86/11/937/09 $1.00
Volume 50 November 1986 937-945

PGH_2, Upjohn Company), causes shape change at concentrations of 6 – 60 nM, reversible aggregation at 110 – 300 nM, and irreversible aggregation at concentrations greater than 600 nM (7). It is reasonable to expect TxA_2 to have similar biological activity.

Thrombin, a serine protease, plays an important role in the coagulation cascade, activating many of the coagulation factors and converting fibrinogen to fibrin. Thrombin also activates platelets independently of fibrin, causing irreversible aggregation at levels of 0.1 to 0.3 units/ml (5). Thrombin is generated enzymatically on the surface of the platelet, where factor Va, factor Xa, and Ca^{2+} combine with platelet phospholipid to form the prothrombinase complex, which converts plasma prothrombin to thrombin. Thrombin may also be generated in the bulk fluid independently of platelets, but the conversion rate is several orders of magnitude greater in the presence of platelet membrane (8).

Thrombin activity is inhibited by the circulating protein antithrombin III (AT III), present in the blood at a concentration of 4 μM (9). The inhibitory activity of AT III is greatly accelerated by heparin, a commonly used anticoagulant and antithrombotic agent. Antithrombin III and heparin do not greatly affect the generation of thrombin, they mainly inactivate it after generation.

The purpose of this paper is to investigate the feasibility of the mechanism for local control of mural thrombogenesis proposed above by solving the equations describing the transport of mass from an idealized thrombus to flowing blood in contact with the thrombus. This allows the estimation of the concentrations that develop in the neighborhood of an individual thrombus releasing and generating these platelet active species.

Similar modeling (10, 11, 12) has been performed for the macroscopic problem, where the generation and release of ADP, TxA_2, and thrombin from platelets accumulating on a collagen-coated surface was seen to persist near the surface in concentrations that could affect platelet function further downstream. This analysis gives little insight, however, into the microscopic problem, which is to consider if the concentrations developing near a particular thrombus could actually affect further aggregation at that same thrombus. The microscopic problem has been previously studied (13), but only in a qualitative sense, to determine the approximate shapes of the concentration contours generated.

FORMULATION OF THE PROBLEM

Consider a fluid flowing in fully developed laminar flow between two parallel plates forming the walls of a thin rectangular channel of width 2B. The fluid enters the channel at $z = -\infty$ with a uniform and zero concentration, C_A, of the species of interest, A. At $z = 0$ the fluid encounters a mass-transfer region, extending from $z = 0$ to $z = L$, where the species of interest is released from the wall at a specified flux, N_A, which has dimensions of moles of A per unit area per unit time. The fluid then proceeds downstream, where no additional mass is released from the wall. Furthermore, consider the possible removal of the active diffusing substance by a first-order bulk phase reaction, A $\rightarrow$ D, where D is some inactive form of A. The physical situation is depicted in Fig. 1.

The diffusion convection equation describing this situation is given by

$$v_z(x)\frac{\partial C_A}{\partial z} = D_{AW}\left[\frac{\partial^2 C_A}{\partial x^2} + \frac{\partial^2 C_A}{\partial z^2}\right] - k\,C_A, \tag{1}$$

where D_{AW} is the translational diffusion coefficient of A in the fluid, k is a first-order reaction rate constant, and $v_z(x)$ is the velocity profile which, for a Newtonian fluid, is given by

$$v_z(x) = v_{max}\left[1 - \left(\frac{x}{B}\right)^2\right]. \tag{2}$$

The boundary conditions for Eq. 1 are given by

$$C_A(x, -\infty) = 0 \tag{3}$$

$$\frac{\partial C_A}{\partial x}(0, z) = 0 \tag{4}$$

$$-D_{AW}\frac{\partial C_A}{\partial x}(B, z) = \begin{cases} N, & 0 \le z \le L \\ 0, & z < 0, z > L. \end{cases} \tag{5}$$

The left hand side of Eq. 1 represents mass transport in the axial direction by convection. The right hand side of Eq. 1 contains the diffusion and bulk phase reaction terms. The second derivative with respect to x represents mass transport perpendicular to the surface (across streamlines) by diffusion. The second derivative with respect to z represents mass transport in the axial direction by diffusion. For most situations, this term has a near zero contribution to the solution, meaning that mass transport in the axial direction is greatly dominated by convection, rather than by diffusion. However, the region of interest in this study is very near the wall, where local fluid velocities are low, even though the average velocity may be high. In this region, the axial diffusion term must be included.

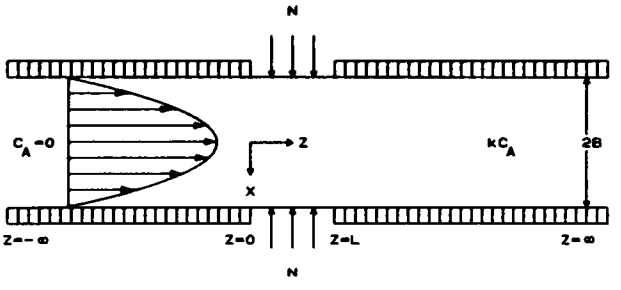

FIGURE 1 Illustration of the mass transfer model, where blood flows by a zone of length L releasing species A at a known flux N. Species A may then be inactivated by a first order reaction in the bulk.

Eq. 1 may be rendered dimensionless by introducing the following variables:

$$\eta = \frac{x}{B}, \qquad \zeta = \frac{z}{B\,Pe}, \qquad \chi = \frac{C_A D_{AW}}{N B}$$

$$\zeta_0 = \frac{L}{B\,Pe}, \qquad Pe = \frac{v_{max} B}{D_{AW}}, \qquad \kappa = \frac{kBPe}{v_{max}}.$$

This yields

$$\frac{\partial \chi}{\partial \zeta} = \frac{1}{1-\eta^2}\left[\frac{\partial^2 \chi}{\partial \eta^2} + \frac{1}{Pe^2}\frac{\partial^2 \chi}{\partial \zeta^2} - \kappa \chi\right], \tag{6}$$

where χ is the dimensionless concentration of species A, ζ is the dimensionless axial position from the beginning of the flux zone, and η is the dimensionless distance from the center of the flow channel. The boundary conditions for Eq. 6 are

$$\chi(\eta, -\infty) = 0 \tag{7}$$

$$\frac{\partial \chi}{\partial \eta}(0, \zeta) = 0 \tag{8}$$

$$\frac{\partial \chi}{\partial \eta}(1, \zeta) = \begin{cases} 1, & 0 \le \zeta \le \zeta_0. \\ 0, & \zeta < 0, \zeta > \zeta_0. \end{cases} \tag{9}$$

The parameter ζ_0 is the dimensionless length of the flux zone, which represents the growing thrombus. The parameter *Pe* is the Peclet number and represents the ratio of mass transport by convection to mass transport by diffusion. The parameter κ is the dimensionless reaction rate constant.

SOLUTION OF THE PROBLEM

This elliptic differential equation, neglecting for the moment the chemical reaction term, is known as the extended Graetz problem with Neumann boundary conditions. It has been solved analytically (14) by decomposing Eq. 8 into two first-order partial differential equations. The result is a series solution of expansion coefficients multiplied by eigenfunctions, with the eigenvalues and eigenfunctions expressed in terms of confluent hypergeometric functions.

In the region of interest in this problem the dimensionless axial positions (ζ) are quite small, typically from 10^{-4} to 10^{-6}. Series solutions of this type are difficult to evaluate for small ζ, as they require the evaluation of many eigenvalues and expansion coefficients. For this reason, it was not possible to utilize this analytical solution in these computations.

Another analytical solution exists, this one derived by applying a double-sided Laplace transform (15). Evaluation of this solution in the region of interest is, however, also not feasible.

Because of the above difficulties, the use of an analytical solution was abandoned and Eq. 6 was solved numerically by collocation using bicubic Hermite elements as the basis functions. The ELLPACK routines (16) were used to perform the computations. A rectangular grid with nonuniform grid spacing was used, with 52 grid lines in the ζ direction and 10 in the η direction.

Computationally, the inlet condition at negative infinity was replaced by the same condition two thrombus lengths upstream of $\zeta = 0$. Numerical solutions for elliptic partial differential equations require a boundary condition on all sides of the problem. For the downstream condition, it was assumed that the axial variation of the concentration was small five thrombus lengths downstream of $\zeta = 0$. Additionally, since the concentration profiles develop only near the wall of the flow chamber, the symmetry condition at the center of the flow chamber was not used. This condition was replaced by assuming that the concentration of species A fell to zero some distance away from the wall. This distance was determined by performing the computations on the simpler parabolic problem that is obtained when the axial diffusion term is neglected. This distance ranged from $\eta = 0.8$ to $\eta = 0.95$, depending on the substance and the wall shear rate. Additional details regarding the numerical method have been published elsewhere (17).

Computations were performed for typical thrombi 10 and 20 μm long in a channel 200 μm wide. The various parameters used in the computations for these two model thrombi are shown in Table I. The data for the sizes and growth rates of the thrombi were derived from experimental measurements taken in our laboratory (18).

The growth rates of individual thrombi on collagen-coated glass in contact with flowing whole blood were measured using epi-fluorescence video microscopy with digital image processing. The growth rates and thrombus sizes in Table I are typical for thrombosis on this substrate. Collagen is a major component in the subendothelial tissue of a blood vessel and serves as a subendothelial model. Thrombosis on vascular subendothelium, as described, for example, in reference one, is very similar to that on collagen-coated glass.

Thrombus growth rates have been seen to depend upon the local wall shear rate (1, 18). This effect is due to the depletion of platelets in the fluid layer near the reactive

TABLE I
PARAMETERS FOR MODEL THROMBI

Thrombus length	Thrombus width	Growth rate	Size	Flux of ADP[11]*	Flux of TxA_2[19]	Flux of thrombin[20]
μm	μm	Plt/s‡	Plt	$mol/\mu m^2\,s$	$mol/\mu m^2\,s$	$units/\mu m^2\,s$§
10	10	0.2	20	$4.5 \cdot 10^{-20}$	$2.3 \cdot 10^{-21}$	$1.5 \cdot 10^{-10}$
20	20	0.8	320	$4.5 \cdot 10^{-20}$	$9.1 \cdot 10^{-21}$	$6.2 \cdot 10^{-10}$

*The superscripts indicate the original references containing the data from which the fluxes were calculated. A description of the flux computations may be found in Appendix I.
‡Plt = Platelets.
§Specific activity 3 units/μg.

surface as the blood flows over the surface. Transport of platelets into the depleted zone depends on the effective platelet diffusivity, which has been shown to be shear rate dependent. This paper considers only small injury sites, that is, the single mural thrombus. Such conditions are likely to be more reasonable under physiological conditions, where large regions of subendothelium are rarely exposed. In the case of a small reactive site, rather than a large one, there is little platelet depeletion, and the thrombus growth rate is not a strong function of wall shear rate.

Three platelet-activating substances were considered, namely, ADP, TxA_2, and thrombin. The flux rates were computed from data given in references 11, 19, and 20 for ADP, TxA_2, and thrombin release and generation by platelets stimulated by collagen. The details of the computations of the fluxes of these three species are contained in Appendix I.

ADP was assumed to be released by the dense granules of each platelet instantaneously as it attached to the growing thrombus, and therefore the flux depended on the growth rate of the thromus, rather than the size of the thrombus. 75% of the granules were assumed to be released. Values in this range are typical for stimulation by collagen.

Thromboxane A_2 is generated enzymatically within the platelet, and therefore the flux depended on the number of platelets in the mural thrombus, rather than the growth rate. Intracellular arachidonic acid, the precursor for TxA_2 production, was assumed not to be depleted. Furthermore, diffusion of TxA_2 produced by the platelets at the bottom of a thrombus through the thrombus before release into the flow stream was not considered. Each platelet was assumed to have equal access to the flow stream. Thus, these generation rates represent an upper bound on the TxA_2 flux.

Thrombin is generated enzymatically on the surface of the platelet, so thrombin flux also depends on the number of platelets composing the thrombus. As was the case for TxA_2, each platelet was assumed to have equal access to the flow stream, so diffusion of prothrombin (reactant) and thrombin (product) through the thrombus was not considered. These assumptions are, therefore, approximations that reflect the limiting case of maximum generation and release of these three platelet-activating substances.

Three bulk phase chemical reactions were considered, namely, the degradation of TxA_2 to TxB_2, the inactivation of thrombin by AT III, and the inactivation of thrombin by AT III accelerated by heparin. The important physical parameters for these species and reactions are shown in Table II.

The diffusion coefficients for ADP and TxA_2 in plasma were estimated by the Wilke-Chang correlation (21). This method requires the knowledge of the molar volume of the solute at its normal boiling point. The group contribution correlation of Le Bas (22) was used to estimate these values. The diffusion coefficient for thrombin in plasma was estimated using a correlation developed for proteins (23). A plasma viscosity of 1.8 centipoise was used in all of these computations.

TABLE II
PARAMETERS FOR PLATELET ACTIVE SPECIES AND CHEMICAL REACTIONS

Species	ADP	TxA_2	Thrombin	AT III	Heparin
MW	424.2	352.5	36600	62000	20000
$D_{AW}(cm^2/s)$*	$2.37 \cdot 10^{-6}$	$2.14 \cdot 10^{-6}$	$4.16 \cdot 10^{-7}$	—	—
$k(s^{-1})$‡	—	0.0161§	—	0.0283‖	267¶

*All of the diffusion coefficients were estimated by correlations in references 21, 22, and 23. The text contains a description of the estimation methods.

‡The pseudo first order reaction rate constants were calculated from data in references 6, 24, and 25 for TxA_2, AT III, and AT III with heparin, respectively. A description of the computation of these values is given in Appendix II.

§For the nonenzymatic hydrolysis of TxA_2 to TxB_2.

‖For the inhibition of thrombin by 4 μM AT III alone.

¶For the inhibition of thrombin by 4 μM AT III accelerated by equimolar heparin.

The reaction rate coefficients were obtained from references 6, 24, and 25 for the degradation of TxA_2 to TxB_2, the inactivation of thrombin by AT III, and the inactivation of thrombin by AT III accelerated by equimolar heparin, respectively.

The assumption was made that the concentration of AT III was large compared with the concentration of thrombin in the neighborhood of a thrombus. Hence, it was not necessary to consider the diffusion of AT III and heparin. Similarly, the assumption was made that the plasma level of prothrombin, the precursor of thrombin, was large compared with the concentration of thrombin developed. Hence, the diffusion of prothrombin to the thrombus before conversion to thrombin was not considered. Justifications for these assumptions are given in the Results section of this paper.

Computations were performed for three wall shear rates, 100, 500, and 1,500 s^{-1}. The lowest value corresponds to a venous shear rate, and the highest value to an arterial shear rate (1).

RESULTS AND DISCUSSION

Important to understanding the effect of the released and generated platelet active substances is a knowledge of the time that a platelet flowing nearby is exposed to these concentrations. The time that a platelet spends directly over the thrombus may be estimated from the parabolic velocity profile. These times are, as one would expect, rather short. For example, a platelet flowing 2 μm from the surface spends approximately 50, 10, and 3.0 ms directly over the 10-μm thrombus for wall shear rates of 100, 500, and 1,500 s^{-1}.

Computations were performed for thrombi 10 and 20 μm long. Results for the former case are given explicitly in

Figs. 2 to 5, and results for the latter thrombus are referred to by comparison with the 10-μm case. The detailed results for the 20-μm-long thrombus may be found elsewhere (12, 17).

Adenosine Diphosphate

The ADP concentration profiles developing in the neighborhood of the 10 μm model thrombus are shown in Fig. 2. The magnitudes of the concentrations that are attained close to the wall are approximately 0.7 μM or less; recall that 0.2 μM ADP is required to cause shape change and reversible aggregation in platelet rich plasma. An increase in the wall shear rate from 100 to 1,500 s^{-1} causes a 2.5 fold-drop in the maximal ADP concentrations. An increase in the size of the thrombus from 10 to 20 μm causes a slight increase in the magnitudes of the concentrations that develop. The reason for this relatively small increase is that the flux of ADP from the surface depends on the rate of granule release from the platelets, which in turn depends on the rate of arrival of platelets to the thrombus. The rate

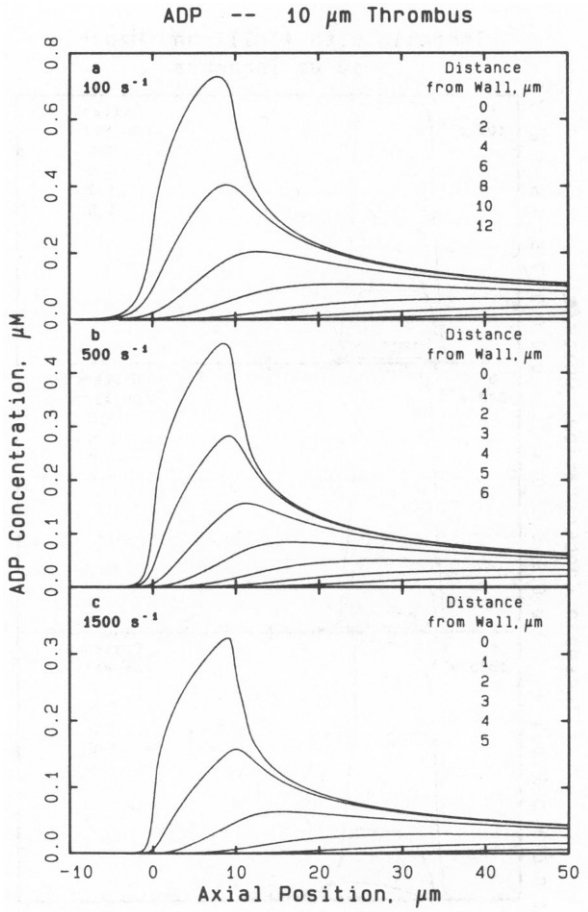

FIGURE 2 Local concentration profiles for adenosine diphosphate (ADP) released from the granules of the platelets in a 10-μm thrombus. Wall-shear rates are (*a*) 100 s^{-1}, (*b*) 500 s^{-1}, and (*c*) 1,500 s^{-1}. The distance from the wall, where the thrombus forms, is varied parametrically, with the top number referring to the top curve, the second referring to the second, and so on.

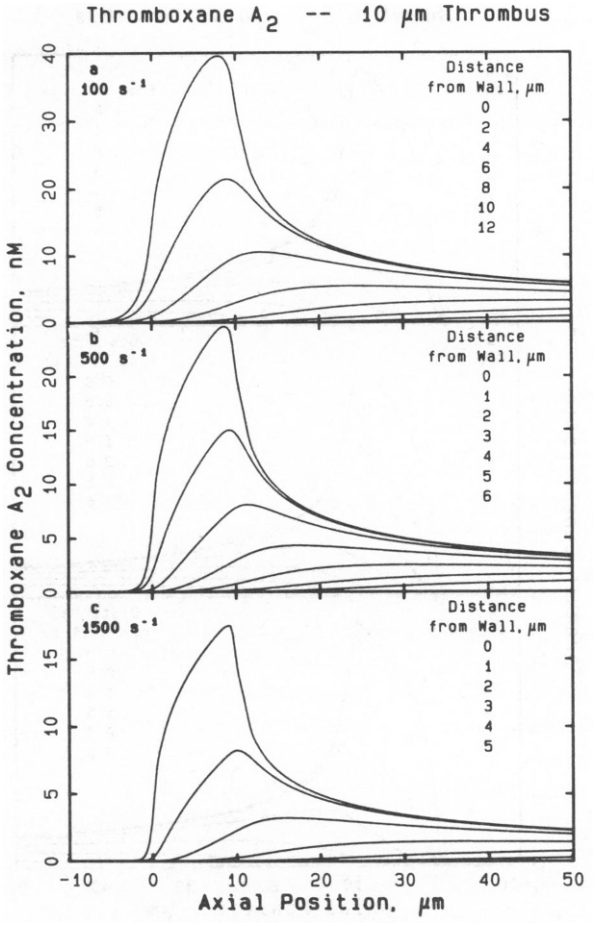

FIGURE 3 Local concentration profiles for thromboxane A_2 produced by the platelets of a 10-μm thrombus. Wall shear rates are (*a*) 100 s^{-1}, (*b*) 500 s^{-1}, and (*c*) 1,500 s^{-1}.

of arrival per unit area is the same for both the large and the small thrombi.

Considering the concentrations computed in the vicinity of the model thrombi, granule released ADP may play some role in the modulation of thrombus growth. It is unlikely, however, that released ADP plays a profound role, since it appears in concentrations not greatly above the threshold for minimal stimulation.

Thromboxane A_2

The TxA_2 concentration profiles computed in the vicinity of the 10 μm-long model thrombus are shown in Fig. 3. The concentrations that develop are 40 nM or less. It is difficult to quantify the biological activity of TxA_2, since it has not yet been successfully purified. For the TxA_2 mimic, U-46619, however, concentrations of 6 – 60 nM and 110 – 300 nM are required to stimulate shape change and reversible aggregation in platelet-rich plasma. An increase in the wall shear rate from 100 to 1,500 s^{-1} results in a 2.5 fold drop in the maximal TxA_2 concentrations. Increasing the size of the thrombus from 10 to 20 μm results in a 5-fold increase in the maximal concentrations. This large

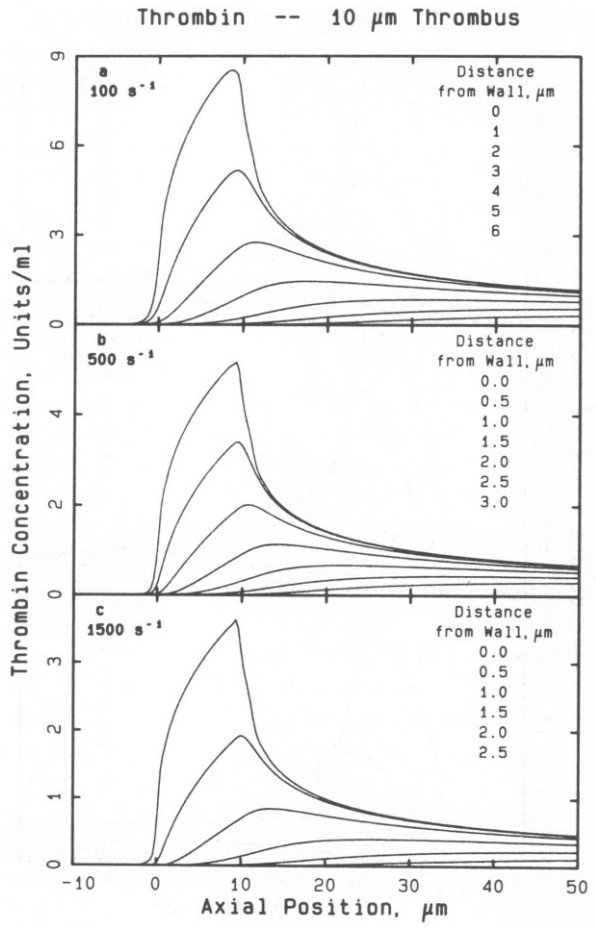

FIGURE 4 Local concentration profiles for thrombin produced by the platelets of a 10-μm thrombus. Wall shear rates are (*a*) 100 s^{-1}, (*b*) 500 s^{-1}, and (*c*) 1,500 s^{-1}.

increase results because the TxA_2 flux at the surface depends not on the rate of platelet arrival to the thrombus, as is the case for ADP, but on the number of platelets that are already present in the thrombus.

It may be that TxA_2 plays an important role in mural thrombus formation at the later stages, when the thrombus is already fairly large. TxA_2 generation would appear, however, to play only a marginally important role in the initial stages of thrombus formation, when the cell aggregate is small.

The fluid phase nonenzymatic hydrolysis of TxA_2 to the biologically inactive TxB_2 was considered and was found to have no effect on the TxA_2 concentrations in the vicinity of the thrombus. This is because its half-life, 43 s, is long when compared with the time that a fluid element spends in the neighborhood of a thrombus.

Thrombin

The thrombin concentration profiles computed in the vicinity of the 10-μm-long model thrombus are shown in Fig. 4. The concentrations that develop near the wall are ≦9 units/ml. The thrombin level required to stimulate platelet activity in platelet rich plasma is much smaller than this value, ~0.1 units/ml. Increasing the wall shear rate from 100 to 1,500 s^{-1} causes an approximately 2.5-fold decrease in the maximal concentrations. Increasing the size of the thrombus from 10 to 20 μm results in a fivefold increase in the thrombin concentrations. This large increase is again because the thrombin flux at the wall depends on the number of platelets that form the thrombus, rather than the rate of arrival of platelets to the thrombus.

It is clear that thrombin generation is likely to play a very important role in the mechanism of mural thrombogenesis. The thrombin concentrations are significantly larger than the minimum required for both the small and the large thrombi, and for both the low and the high shear rate cases. It is likely that thrombin plays an important role by both directly stimulating platelet activation and by structurally stabilizing the growing thrombus by catalyzing fibrin formation.

The enzymatic inactivation of thrombin by antithrombin III, in the absence of heparin, as would be found in the

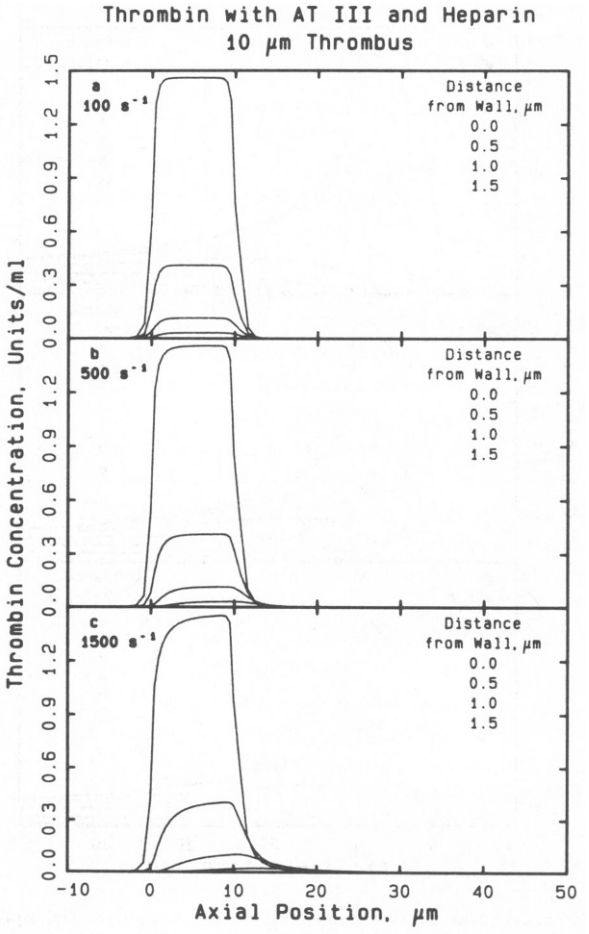

FIGURE 5 Local concentration profiles for thrombin produced by the platelets of a 10-μm thrombus with bulk phase inactivation by antithrombin III accelerated by heparin. Wall shear rates are (*a*) 100 s^{-1}, (*b*) 500 s^{-1}, and (*c*) 1,500 s^{-1}.

unaltered physiological case, was seen to have little effect on the local thrombin concentrations that develop in the vicinity of the thrombi.

In the altered physiological case, however, when the AT III accelerator heparin has been introduced, very significant inhibition of local thrombin activity was seen. This case is shown in Fig. 5. Concentrations that develop are $\leq$1.5 units/ml for the 10-μm-long thrombus. Variation of the wall shear rate was seen to have very little effect on the concentration profiles, because of the rapid inactivation near the surface. Variation of the size of the thrombus from 10 to 20 μm resulted in a fivefold increase in the active thrombin concentration.

Although the addition of heparin to the system resulted in great inactivation of thrombin, it is likely that these reduced concentrations are still large enough to stimulate platelet activation. In addition, thrombus stabilization by fibrin formation would almost surely still be significant.

The assumption was made in this mathematical analysis that the thrombin concentrations were small relative to that of AT III. Hence, the diffusion of AT III was not considered. This assumption was valid, since the largest thrombin concentration, 42 units/ml or 0.38 μM, is still one order of magnitude less than the AT III concentration, 4 μM.

Likewise, the assumption that prothrombin was also present in sufficient excess was also reasonable. Prothrombin is present in plasma at levels of approximately 1.0 μM, about three times the largest thrombin concentration calculated.

Comments

It should be kept in mind when interpreting these results that some platelet stimulating agents act synergistically, that is, that subthreshold levels of one agent present with subthreshold levels of another agent can cause platelet activation. Thus, for example, TxA_2 generation may be more important than it seems at first glance, for it may potentiate the ability of platelets to respond with greater sensitivity to some of the other aggregatory agents.

The transport model calculations suggest that the "active cloud" of platelet active substances surrounding a growing thrombus can provide a mechanism to explain the elongated morphology and distal growth seen in model vessels in contact with flowing whole blood (3). Thrombin appears to be of profound importance, with a lesser but perhaps still significant role for TxA_2 and ADP.

This model does not account for flow disturbances caused by the thrombus; the thrombus was considered to be flush with the wall of the flow channel. This is reasonable for small thrombi. Regions of recirculation might exist immediately downstream from larger thrombi if flow disturbances were accounted for. If this were to be the case, then even higher concentrations of the platelet active species might be present near the distal side of the thrombus.

This paper considers only the local contribution of the generation and release of these platelet active substances to the activation of platelets flowing near the surface and their subsequent recruitment to the growing thrombus. It does not attempt to assess the macroscopic effect of release from many of these thrombi lumped together, which has been addressed elsewhere (12). The local consideration attempts to understand why platelets add onto a growing thrombus at its distal end, whereas the macroscopic consideration attempts to access the role of upstream release on downstream thrombosis.

The behavior of blood platelets at a blood-material interface depends largely on the nature of the material, that is, on the stimulation of the platelets induced by contact with the material. In the case of the contact of blood with subendothelium, large mural thrombi form. One might expect similar behavior on atheromatous plaques. Mural thrombogenesis on an artificial polymeric material depends on the type of polymer and method of processing.

The computations contained herein are for the contact of blood with collagenous surfaces, e.g., model subendothelium. The rates of granule release and thromboxane A_2 generation were taken from the literature were collagen was used as the stimulatory agent. The results show that for this material the release of granule bound ADP may be marginally important in mural thrombogenesis. TxA_2 generation may be important in mural thrombgenesis, particularly in the propagation of larger thrombi. The synthesis of thrombin on the surface of the platelet is probably very important, and thrombin is significantly inactivated by the addition of heparin. However, sizable concentrations of thrombin still exist in the vicinity of the thrombus even when heparin is used.

In the case of synthetic polymeric surfaces, such as those used in artificial organs or blood-contacting devices, experiments must be performed to determine the rates of release and generation of these platelet active substances before this analysis can be quantitatively applied to estimate these concentrations near growing thrombi.

APPENDIX I

Flux Computations

The fluxes of the platelet active substances were estimated from a knowledge of the generation rate per platelet and the number of platelets in the model thrombus or the rate of growth of the thrombus. The details of the flux computations are shown below for the 10-μm-long thrombus case. Assumptions made give maximum wall fluxes of each compound. Therefore the fluid concentrations represent an upper bound on those obtained experimentally.

ADP Flux

The ADP flux was estimated assuming that 75% of the dense granule contents are released immediately upon platelet attachment to the growing thrombus (11). This value is typical for platelet stimulation by

collagen. A single platelet contains $3.0 \cdot 10^{-17}$ moles of dense granule bound ADP (11). Assuming a growth rate of 0.2 platelets/s (from our experimental data on collagen [12, 17, 18]) over a thrombus area of 100 μm^2, one may calculate the flux as

$$\text{Flux}_{ADP} = \frac{(0.2 \text{ plt/s})(3.0 \cdot 10^{-17} \text{ mol/plt})(0.75)}{100 \ \mu m^2}$$

$$= 4.5 \cdot 10^{-20} \text{ mol}/\mu m^2 \text{ per s.}$$

Thromboxane A_2 Flux

Thromboxane A_2 is generated enzymatically intracellularly near the membrane of the platelet. In reference 19 thromboxane B_2 generation rates were measured for platelets stimulated by collagen in platelet-rich plasma. Since TxA_2 is rapidly converted into TxB_2, this data may be taken as a measure of TxA_2 generation. Fig. 3 *a* of this reference shows the production of 110 ng/ml of TxB_2 during the 75-s-long ascending phase of the aggregation stimulated by 15 μg/ml collagen. Platelets were present at 440,000/μl, so the generation rate was approximately $4 \cdot 10^{-18}$ ng/plt per s or $1.1 \cdot 10^{-20}$ mol/plt per s. Assuming that the thrombus consists of 20 platelets and has an area of 100 μm^2, one may calculate the flux as

$$\text{Flux}_{TxA_2} = \frac{(20 \text{ plt})(1.1 \cdot 10^{-20} \text{ mol/plt/s})}{100 \ \mu m^2}.$$

$$= 2.3 \cdot 10^{-21} \text{ mol}/\mu m^2 \text{ per s}$$

Thrombin Flux

Thrombin is generated enzymatically on the extracellular side of the platelet membrane where factor Va, factor Xa, platelet phospholipid, and Ca^{2+} combine to form the prothrombinase complex. This complex converts plasma prothrombin to thrombin. In reference 20, thrombin generation rates were measured in the presence of platelets and physiologic concentrations of prothrombin. Under rate saturating concentrations of factor Xa, which were less than physiologic, the thrombin generation rate was 4.6 units/ml per min for a reaction mixture containing $1 \cdot 10^8$ platelets/ml. This is equivalent to $7.7 \cdot 10^{-10}$ units/platelet per s. Again assuming that the thrombus consists of 20 platelets and has an area of 100 μm^2, the flux may be calculated as

$$\text{Flux}_{Thrombin} = \frac{(20 \text{ plt})(7.7 \cdot 10^{-10} \text{ units/plt/s})}{100 \ \mu m^2}.$$

$$= 1.5 \cdot 10^{-10} \text{ units}/\mu m^2 \text{ per s}$$

APPENDIX II

Reaction Rate Constant Computations

The details of the computation of the pseudo first order reaction rate constants for the three bulk-phase inactivation reactions are given below.

Hydrolysis Of Thromboxane A_2

Thromboxane A_2 is hydrolyzed nonenzymatically in aqueous solution to thromboxane B_2, which is biologically inactive. The half life of this first order reaction is 43 s (6). The reaction rate constant may be calculated as $k_{TxA_2} = -[\ln(1/2)]/43 \text{ s}) = 0.0161 \text{ s}^{-1}$.

Inactivation Of Thrombin By AT III

Thrombin is inactivated by antithrombin III, which was assumed to be present in the plasma at a concentration of 4.0 μM. The second order reaction rate constant was taken directly from reference 24 as $k'' = 4.25 \cdot 10^5 \text{ M}^{-1} \text{ min}^{-1}$, where the form of reaction rate equation was $-d[T]/dt = k''[AT][T]$, where [T] is thrombin concentration and [AT] is antithrombin III concentration. A pseudo first order reaction rate constant may be calculated by assuming an antithrombin III concentration, which was chosen as 4 μM. One obtains a value for $k_{thr,AT\,III}$ of 0.0283 s^{-1}.

Inactivation Of Thrombin By AT III With Heparin

The inactivation of thrombin by AT III is greatly accelerated by the anticoagulant heparin. Heparin concentration was assumed to be equimolar with AT III, 4.0 μM or ~2.0 μg/ml. Table II in reference 25 gives the second order reaction rate constant as a function of heparin concentration. The data presented in reference 25 was for heparin concentrations much lower than 2.0 μg/ml. The data were extrapolated to obtain an estimate of $4.0 \cdot 10^9 \text{ M}^{-1} \text{ min}^{-1}$. The pseudo first order reaction rate constant may be calculated, using the AT III concentation, as $k_{thr,AT\,III,hep} = 267 \text{ s}^{-1}$.

This research was supported by grants HL 18676 and HL 17437 from the National Institutes of Health and grant C-938 from the Robert A. Welch Foundation.

Received for publication 2 December 1985 and in final form 7 April 1985.

REFERENCES

1. Turitto, V. T., and H. R. Baumgartner. 1982. Platelet-surface interactions. *In* Hemostasis and Thrombosis: Basic Principles and Clinical Practice. R. W. Colman, J. Hirsh, V. J. Marder, and E. W. Salzman, editors. J. B. Lippincott Company, Philadelphia. 364–379.
2. Anderson, J. M., and K. Kottke-Marchant. 1985. Platelet interactions with biomaterials and artificial devices. *CRC Crit. Rev. Biocompat.* 1:111–204.
3. Adams, G. A., S. J. Brown, L. V. McIntire, S. G. Eskin, and R. R. Martin. 1983. Kinetics of platelet adhesion and thrombus growth. *Blood.* 62:69–74.
4. Adams, G. A., L. V. McIntire, R. R. Martin, J. D. Olson, and H. Sybers. 1982. The effects of heparin and polymorphonuclear neutrophil leukocytes on platelet aggregate formation on collagen-coated tubes. *Trans. Am. Soc. Artif. Intern. Organs.*28:444–448.
5. Weiss, H. J. 1982. Platelets: Pathophysiology and Antiplatelet Drug Therapy. Alan R. Liss, Inc., New York. 165 pp.
6. Hammarstrom, S., J. A. Lindgren, and P. Roos. 1979. Biosyntheses of prostaglandins and thromboxanes. *In* Chemistry, Biochemistry and Pharmacological Activity of Prostanoids. S. M. Roberts and F. Scheinmann, editors. Pergamon Press, Oxford. 221–232.
7. Jones, R. L., N. H. Wilson, and C. G. Marr. 1979. Thromboxane-like activity of prostanoids with aromatic substituents at C16 and C17. *In* Chemistry, Biochemistry and Pharmacological Activity of Prostanoids. S. M. Roberts and F. Scheinmann, editors. Pergamon Press, Oxford. 210–220.
8. Nesheim, M. E., J. B. Taswell, and K. G. Mann. 1979. The contribution of bovine Factor V and Factor Va to the activity of prothrombinase. *J. Biol. Chem.*254:10952–10962.
9. Harpel, P. C. 1982. Blood proteolytic enzyme inhibitors: their role in modulating blood coagulation and fibrinolytic enzyme pathways. *In*Hemostasis and Thrombosis: Basic Principles and Clinical Practice. R. W. Colman, J. Hirsh, V. J. Marder, and E. W. Salzman, editors. J. B. Lippincott Company, Philadelphia. 738–747.
10. Adams, G. A., and I. A. Feuerstein. 1981. Platelet adhesion and release: interfacial concentration of released materials. *Am. J. Physiol.* 240:H99–H108.
11. Adams, G. A., and I. A. Feuerstein. 1983. Maximum fluid concen-

trations of materials released from platelets at a surface. *Am. J. Physiol.* 244:H109–H114.

12. Hubbell, J. A., and L. V. McIntire. 1986. Visualization and analysis of mural thrombogenesis on collagen, polyurethane, and nylon. *Biomaterials.* In press.
13. Butruille, Y. A., E. F. Leonard, and R. S. Litwak. 1975. Platelet-platelet interactions and non-adhesive encounters on biomaterials. *Trans. Am. Soc. Artif. Intern. Organs.* 21:609–614.
14. Papoutsakis, E., D. Ramkrishna, and H. C. Lim. 1980. The extended Graetz problem with prescribed wall flux. *AIChE J.* 26:779–787.
15. Jones, A. S. 1972. Two-dimensional adiabatic forced convection at low Peclet number. *Appl. Sci. Res.*25:337–348.
16. Rice, J. R., and R. F. Boisovert. 1985. Solving Elliptic Problems Using ELLPACK. Springer-Verlag, New York. 497 pp.
17. Hubbell, J. A. 1986, Visualization and Analysis of Mural Thrombogenesis. Ph.D. thesis. Rice University. Houston, TX. 172 pp.
18. Hubbell, J. A., and L. V. McIntire. 1985. A technique for visualization and analysis of mural thrombogenesis. *Rev. Sci. Instrum.* 57:892–897.
19. De Caterina, R., D. Giannessi, P. Gazzetti, and W. Bernini. 1984. Thromboxane-B_2 generation during ex-vivo platelet aggregation. *J. Nucl. Med. All. Sci.* 28:185–196.
20. Miletich, J. P., C. M. Jackson, and P. W. Majerus. 1978. Properties of the Factor XA binding site on human platelets. *J. Biol. Chem.* 253:6908–6916.
21. Bird, R. B., W. E. Stewart, and E. N. Lightfoot. 1960. Transport Phenomena. John Wiley & Sons, New York. 780 pp.
22. Reid, R. C., J. M. Prausnitz, and T. K. Sherwood. 1977. The Properties of Gases and Liquids. McGraw-Hill, Inc., New York. 688 pp.
23. Young, M. E., P. A. Carroad, and R. L. Bell. 1980. Estimation of diffusion coefficients of proteins. *Biotechnol. Bioeng.* 22:947–955.
24. Rosenberg, R. D. 1982. Heparin-Antithrombin system. *In* Hemostasis and Thrombosis: Basic Principles and Clinical Practice. R. W. Colman, J. Hirsh, V. J. Marder, and E. W. Salzman, editors. J. B. Lippincott Company, Philadelphia. 962–985.
25. Griffith, M. J. 1982. Measurement of the heparin enhanced-antithrombin III/thrombin reaction rate in the presence of synthetic substrate. *Thrombosis Res.* 25:245–253.